Reduction in ultimate strength capacity of corroded ships involved in collision accidents

Ships and Offshore Structures

ISSN: 1744-5302 (Print) 1754-212X (Online) Journal homepage: http://www.tandfonline.com/loi/tsos20

Reduction in ultimate strength capacity of corroded ships involved in collision accidents

Jonas W. Ringsberg, Zhiyuan Li, Erland Johnson, Artjoms Kuznecovs & Roozbeh Shafieisabet

To cite this article: Jonas W. Ringsberg, Zhiyuan Li, Erland Johnson, Artjoms Kuznecovs & Roozbeh Shafieisabet (2018) Reduction in ultimate strength capacity of corroded ships involved in collision accidents, Ships and Offshore Structures, 13:sup1, 155-166, DOI: 10.1080/17445302.2018.1429158

To link to this article: https://doi.org/10.1080/17445302.2018.1429158

SHIPS AND OFFSHORE STRUCTURES
2018, VOL. 13, NO. S1, S155–S166
https://doi.org/10.1080/17445302.2018.1429158

Taylor & Francis
Taylor & Francis Group

Reduction in ultimate strength capacity of corroded ships involved in collision accidents

Jonas W. Ringsberg [a], Zhiyuan Li [a], Erland Johnson [b], Artjoms Kuznecovs [a] and Roozbeh Shafieisabet [a]

[a]Department of Mechanics and Maritime Sciences, Chalmers University of Technology, Gothenburg, Sweden; [b]Department of Safety – Mechanics Research, RISE Research Institutes of Sweden, Borås, Sweden

ABSTRACT

The objective of the study is to investigate the effects of sudden damage, and progressive deterioration due to corrosion, on the ultimate strength of a ship which has been collided by another vessel. Explicit finite element analyses (FEA) of collision scenarios are presented where factors are varied systematically in a parametric study, e.g. the vessels involved in the collision, and consideration of corroded ship structure elements and their material characteristics in the model. The crashworthiness of the struck ships is quantified in terms of the shape and size of the damage opening in the side-shell structure, and the division of energy absorption between the striking and struck ships for the different collision simulations. The ultimate strength of the struck ship is calculated using the Smith method and the shape and size of the damage openings from the FEA. In conclusion, the study contributes to understanding of how corroded, collision-damaged ship structures suffer significantly from a reduction in crashworthiness and ultimate strength, how this should be considered and modelled using the finite element method and analysed further using the Smith method.

ARTICLE HISTORY
Received 2 October 2017
Accepted 12 January 2018

KEYWORDS
Corrosion; parametric study; ship–ship collision; Smith method; ultimate strength

1. Introduction

Safety of maritime operations is one among several prioritised research areas in the maritime industry, where crashworthiness assessment of ships and offshore structures is a field with high research activity. With an ever-increasing worldwide ship traffic, larger ship sizes and increased number and different types of marine structures offshore, there is an enhanced risk for collision accidents with, for example, wind/wave/tidal energy farms, structures for oil and gas extraction or other ships. Many of these marine structures have been in operation for many years. Corrosion, permanent deformations and accumulated fatigue damage are some factors that influence their residual strength and structural integrity. This investigation focuses on structural integrity analysis that refers to the accidental and ultimate limit states (ULS) of corroded ship structures that are damaged by another vessel.

In conventional ship design practice, it is required to carry out an assessment of a ship's structural and ultimate strength under intact conditions (i.e. no damage opening in the side-shell). In case of a collision accident, where a damage opening occurs in the struck ship's side-shell structure, the safety margin against the ultimate limit strength is greatly reduced due to the damaged condition. An ultimate strength analysis of a damaged ship from a collision accident needs a description of the collision location, shape, size and extent of the ship structure's damages in order to make a reliable estimation of the ship's reserve strength.

Considerable research efforts have been spent on the structural response during collision as well as on the residual ultimate strength of struck ships. Examples of such investigations where the representation of the material and its characteristics can be found in AbuBakar and Dow (2016), Ehlers (2010), Ehlers and Østby (2012), Hogström and Ringsberg (2012), Hogström et al. (2009), Marinatos and Samuelides (2015), Samuelides (2015), Storheim, Amdahl, and Martens (2015), Storheim, Alsos, et al. (2015), Yamada (2014), and Zhang and Pedersen (2017). Faisal et al. (2016) studied the hull collapse strength of double hull oil tankers after collisions using a statistical approach. Several parameters were considered such as impact location, extent of damage (represented by penetration depth in the struck ship) and the collision scenario. Simplified shapes of the structural damages were used in the study. The ship's physical condition due to, e.g. corrosion is also important to consider in this regard. Campanile et al. (2015) present a study on the same topic and type of damage but for bulk carriers including the effect from corrosion using a corrosion model proposed by Paik et al. (2003). The results show how the influence from corrosion of the material leads to a significant decrease in the residual ultimate strength index (RSI). There are several investigations on the buckling ultimate strength, which support this finding for intact structures that suffer from either minor or major corrosion wastage; see e.g. Paik et al. (2009) and Saad-Eldeen et al. (2011).

There are few studies in the literature which systematically present the negative consequences of corrosion on the collision resistance. The influence from corrosion is typically simplified by removing the extra corrosion margin in the damage assessment; see Ringsberg et al. (2017). The objective of the current investigation is to study the effects of sudden damage (ship–ship collision), and progressive deterioration due to

CONTACT Jonas W. Ringsberg Jonas.Ringsberg@chalmers.se

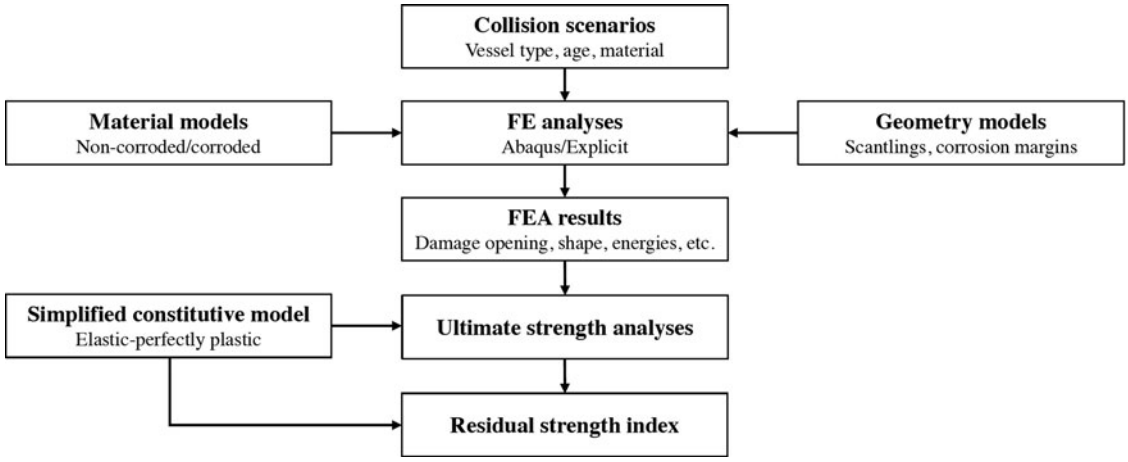

Figure 1. Flowchart of the analysis procedure of the current study.

corrosion, on the ultimate strength of a ship which has been collided by another vessel. The influence from corrosion is considered here by three factors: reduction of the thickness of the ship structure's elements due to corrosion, increased friction coefficient on corroded surfaces and change of the material characteristics of a corroded material as compared with a non-corroded material using the approach presented in Garbatov et al. (2014, 2016). The crashworthiness of non-corroded and corroded struck ships is quantified in terms of the shape and size of the damage opening in the side-shell structure. Explicit finite element (FE) analyses are presented where several factors such as the collided ship type, the corrosion margin thickness and material characteristics are varied systematically in a parametric study. The striking ship is represented by a coastal tanker while the struck ship is either a RoPax ship, or a coastal oil tanker vessel. The ultimate strength of the struck ship is calculated using the Smith method.

Section 1.1 presents the analysis procedure of ultimate strength capacity of ship structures used in the study. Section 2 presents the case study vessels, their FE models, the stress–strain curves (constitutive models) of the non-corroded and corroded materials, and other model details. In the following section, the results from the analyses are presented with emphasis on the influence from corrosion on a damage opening's shape and size, and the struck ship's residual strength. The conclusions of the study are presented in Section 4.

1.1. Methodology

In this study, a methodology has been developed for the assessment of the structural integrity of aged ships that have been damaged during a ship–ship collision accident. An ultimate strength analysis of a damaged ship from a collision accident needs a description of the collision location on the hull, shape, size and extent of the ship structure's damages in order to make a reliable estimation of the ship's reserve strength. It is known that a ship's physical condition due to, e.g. corrosion is important to include in ULS analyses, and this study shows the importance of including it also in accidental limit state (ALS) analyses. Figure 1 presents a flowchart showing how the analyses have been carried out in the study.

The methodology is used in a parametric study of collision scenarios and ship conditions for two case study vessels. Geometrically, the two ship types have different requirements for the allowed loss of material due to corrosion in the cross-section related to the age of the ship. Different stress–strain curves – constitutive models as well as damage models – for non-corroded and corroded materials are accounted for in the nonlinear FE analyses of the ship–ship collision scenarios. The location, shape and size of the damage opening in the struck ship are calculated and used in the Smith method to estimate the ship's ultimate strength as the ultimate vertical bending moment, and the residual strength index (RSI).

2. Case study vessels and finite element analyses

The collision scenario in the study was a collision between two similar-sized vessels. The striking ship was a coastal product/chemical tanker with a total displacement of 10,800 metric tons, in the following referred to as the striking tanker. Two different struck ships were studied for comparison: one RoPax ship and one coastal oil tanker; see Table 1 for their main particulars.

Figure 2 presents the mid-ship section scantlings of the struck ships which are collided amidships by the striking tanker; see Table 2 for the gross scantlings. The RoPax ship is a coastal RoRo cargo vessel with a typical side-shell structure with small distance between the inner and the outer side-shells, which makes the ship sensitive to collision damage (Karlsson 2009). It has three RoRo decks, one on the tank top, one on the main deck and one outdoors on the upper deck. The ship is longitudinally stiffened above the main deck and in the double bottom, and it has a transversely stiffened double side-shell. The spacing between deck beams is 2.4 m. The double side-shell and double bottom structures also act as water ballast tanks. The coastal oil

Table 1. Main data of the struck ships.

	RoPax	Coastal oil tanker
Deadweight (tons)	1700	11,500
Design draught (m)	4	7.4
LOA (m)	88	137.6
Beam (m)	13.3	21.5

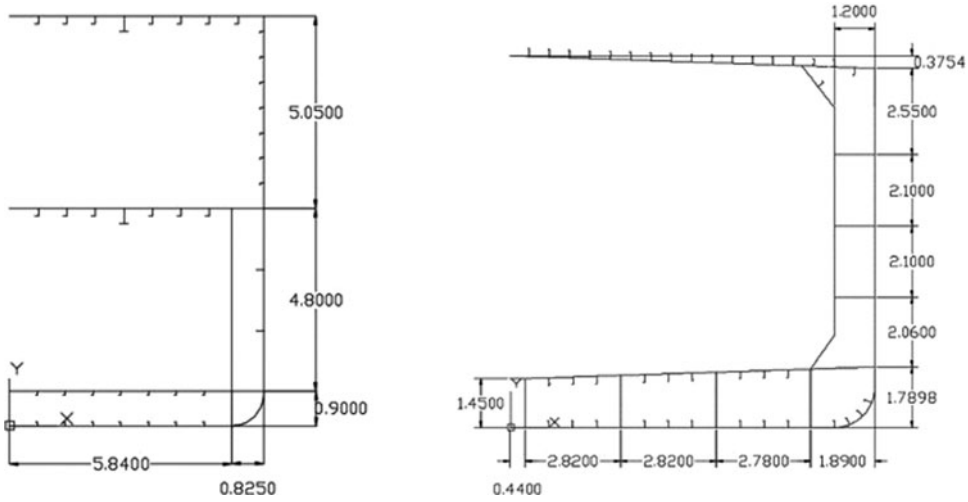

Figure 2. The mid-ship section of the struck ships (unit: meters): (left) the RoPax ship, and (right) the coastal oil tanker.

tanker has longitudinally stiffened double bottom and weather deck, while the double side-shell structure is transversely stiffened. It has a corrugated longitudinal bulkhead in the centre plane of the cross-section. The corrugation is vertical; hence, the bulkhead may be omitted in the ultimate strength calculations since it does not contribute effectively to the hull girder longitudinal strength (IACS 2017).

2.1. Description of FE models

The FE analyses were carried out using the software Abaqus/Explicit ver. 6.13-3 (Abaqus 2016). A thorough presentation of the design of the FE models for collision simulations, description of material characteristics and damage modelling can be found in previous work by the authors; see Hogström and Ringsberg (2012, 2013) for detailed descriptions. Figure 3 presents the geometry of the inner structure of the bulbous bow section of the striking tanker, and the geometries of the struck RoPax and coastal oil tanker ships.

The FE models of the struck ships were made sufficiently large to ensure there was no influence from the boundary conditions on the numerical solution, and the calculated shape and size of the damage opening. The collision impact was always amidships and between bulkheads and web frames. The bow section of the striking tanker was modelled as a deformable bow and restricted to only move in a prescribed direction, which in the current study was a right-angle collision. Other collision

Table 2. Gross scantlings of the structural elements for the RoPax ship and the coastal oil tanker.

RoPax ship	Gross scantling (mm)	Coastal oil tanker	Gross scantling (mm)
Bottom and bilge	10.0	Double bottom longitudinal girders	10.0
Double bottom girder	7.0	Double bottom side-shell frame	13.0
Double bottom side-shell frame	10.0	Double side stringers	9.0
Double side-shell stringer	9.0	Double wall side-shell bottom stiffener	16.0
Double wall horizontal stiffener	10.0	Double wall side-shell middle stiffener	9.0
Double wall side-shell frame	7.0	Double wall side-shell top stiffener	16.0
Double wall side-shell frame appendage	10.0	Inner bottom	12.0
Inner shell	7.0	Inner bottom longitudinal flange	20.0
Lower wheel deck	9.0	Inner bottom longitudinal web	10.0
Main wheel deck	12.0	Inner shell	11.0
Outer shell	14.0	Inner shell longitudinal flange	20.0
Transverse girder flange	20.0	Inner shell longitudinal web	10.0
Transverse girder web	8.0	Inner shell, 3 m below top of tank	15.0
Transverse middle stiffener flange	9.0	Inner shell, tank bottom	13.0
Transverse middle stiffener web	4.5	Outer bottom and bilge	11.0
Upper single side-shell	7.0	Outer bottom and bilge longitudinal flange	20.0
Upper wheel deck	12.0	Outer bottom and bilge longitudinal web	10.0
		Outer shell	11.0
		Outer shell, ice belt	13.0
		Sheer strake	11.0
		Transverse middle stiffener flange	20.0
		Transverse middle stiffener web	10.0
		Weather deck	11.0
		Weather deck longitudinal flange	20.0
		Weather deck longitudinal web	10.0
		Weather deck transverse girder	10.0

Figure 3. The geometry of the inner structure of: (left) the bulbous bow section (i.e. the striking tanker ship), the outer shell of the side-shell structure of (middle) the RoPax ship and (right) the coastal oil tanker.

angles have been investigated by Ringsberg et al. (2017) and have been found to have a significant influence on the damage of the struck ship. The striking ship was given an initial forward velocity of seven knots, while the side-shell structure of the struck ships was held fixed in its circumference (i.e. zero speed). The velocity of the striking bow decreased gradually during the collision event as energy was dissipated through deformations and fracture in the structures. The FE analysis was interrupted when the striking ship's speed had slowed down to zero knots.

The FE meshes were made of four-node shell elements with reduced integration (S4R in Abaqus/Explicit) and five section points through the thickness; however, some triangular elements (S3R in Abaqus/Explicit) were also used. A convergence analysis for the explicit FE analysis was carried out, which resulted in a mesh with finite elements having size of 60 mm. The element length/thickness ratio was 5 in the part of the model with the highest sheet thickness. Time integration was accomplished utilising the explicit time stepping scheme combined with an automatic choice of time step. The general contact condition criterion in Abaqus/Explicit was used in conjunction with a friction coefficient of 0.3 or 0.5 (non-corroded or corroded surface) to model the contacts between surfaces that occur in the collision.

Table 3. Material parameters used in the constitutive material and damage models.

Parameter	NVA virgin (non-corroded)	NVA minorly corroded	NVA severely corroded
Young's modulus, E (GPa)	210	179	158
Poisson's ratio, υ (-)	0.3	0.3	0.3
(Static) Yield stress, $\sigma_{y,s}$ (MPa)	310	310	291
Ultimate tensile strength (MPa)	579	518	440
Hardening coefficient, K (MPa)	616	845	752
Hardening exponent, n	0.23	1.00	1.00
Necking strain, ε_n (%)	23.0	–	–
Fracture strain, ε_f (%)	35.1	24.8	20.0
Cowper–Symonds constant, C (-)	40.4	–	–
Cowper-Symonds constant, P (-)	5	–	–
DE parameters, bilinear model; see Abaqus (2016) for details	(0, 0), (0.02, 0.00458), (1, 0.01832)	–	–

2.2. Description of constitutive material and damage models

The two most important factors that have a big impact on strength reduction in addition to the net section area loss are, according to Garbatov et al. (2016), the change in material parameters caused by corrosion and stress concentration due to local corrosion pits. Several investigations in the literature have studied how the strength capacity of corroded metal structures is affected by the combination of several factors such as the degree of degradation, geometric modelling of pit density and initial imperfections in simulation models used for nonlinear FE analysis; see e.g. Paik et al. (2008) and Paik and Melchers (2008). In the current study, another approach presented by Garbatov et al. (2014, 2016) is used. It is based on stress–strain curve modelling in nonlinear FE analysis of structures subjected to corrosion deterioration, and possibly also maintenance actions. In their approach, an engineering-based approach with a 'phenomenological model' is proposed where the material properties in the constitutive model used to describe a material in the FE analysis are changed to match empirical data obtained from a number of standard tensile tests of the material. Note that this approach does not model a change in the mechanical properties of a corroded material due to changes of the material's chemical compositions. Instead, it is used to describe how a corroded structure's stress–strain characteristics are altered as a consequence of corrosion and the effects thereof. The advantage with the approach is that it is practical to be used in the numerical analysis of large to full-scale models of corroded marine structures; different stress–strain curves can be directly implemented in the FE model using a constitutive material model which describes the stress–strain relationships. In the current study, three different representations of a DNV Grade A (NVA) shipbuilding mild steel were used depending on the grade of corrosion (ship's age and severity of corrosion): NVA virgin (non-corroded), NVA minorly corroded and NVA severely corroded; see Table 3 for a summary of all material parameters for these materials.

The virgin NVA material was represented by a nonlinear elastic–plastic constitutive material model where the isotropic hardening of the inelastic stress–strain relation follows the well-known power law in Equation (1) relating the true stress, σ_{true}, to the true strain, $\varepsilon_{\text{true}}$. The influence from strain rate effects was considered using the Cowper–Symonds relationship in Equation (2), where $\sigma_{y,d}$ is the dynamic yield stress, $\sigma_{y,s}$ is the static yield stress, $\dot{\varepsilon}$ is the material strain rate, and C and P are constants of the Cowper–Symonds relation. Two models were

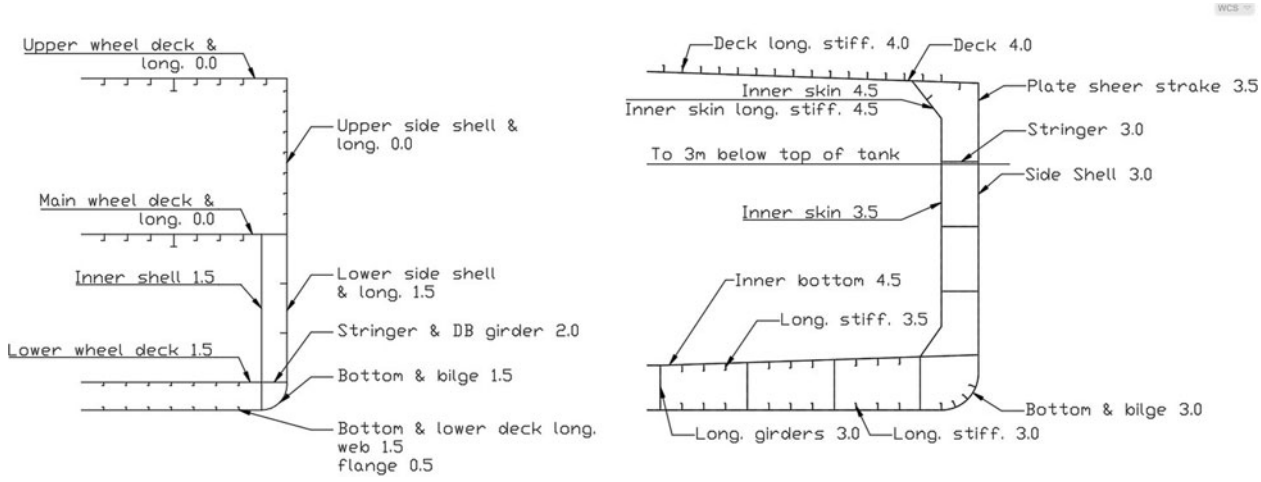

Figure 4. Corrosion margins (unit: mm) for (left) the RoPax ship, and (right) the coastal oil tanker.

combined to represent the material characteristics for failure and degradation leading to fracture: a model for onset of failure (damage initiation, DI) and a model for damage degradation (damage evolution, DE). The shear criterion in Abaqus/Explicit is used to model DI. It is a phenomenological representation of the initiation of damage due to shear band localisation and it uses the equivalent plastic strain according to von Mises at the onset of necking, ε_n. In the post-necking region, the element size of the mesh has a significant influence on the numerical solution. This length dependence between element size and fracture strain has to be accounted for when the DE law is defined. In Hogström et al. (2009), it is shown that Barba's law is applicable in relating the element size to the fracture strain and it has also been used in the current study. Thus, in the current analysis, the shear criterion is used to initiate damage (DI) at the point of necking and it is followed by a bilinear law for DE up to the point of fracture, ε_f, in accordance with the recommendations made in Hogström et al. (2009).

$$\sigma_{\text{true}} = K(\varepsilon_{\text{true}})^n \tag{1}$$

$$\sigma_{y,d} = \sigma_{y,s}(1 + (\dot{\varepsilon}/C)^{1/P}) \tag{2}$$

The constitutive material parameters for the minorly and severely corroded NVA steels were obtained from Garbatov et al. (2014). Both materials were represented by a bilinear elastic–plastic constitutive material model, where the isotropic hardening of the inelastic stress–strain relation between the yield and ultimate tensile stresses was linear. As found in Garbatov et al. (2014), a corroded material is less ductile compared to a non-corroded material, and the necking point is not easily observed during tensile tests. Hence, the damage model of the corroded materials was represented solely by the shear failure criterion in Abaqus/Explicit without any DE law. Further, due to lack of material data in the Cowper–Symonds relationship for corroded materials, it was not accounted for in these materials. In future work, it is recommended to investigate the viscoplastic strengthening and DE characteristics of corroded steel materials.

2.3. Corroded ship structure: corrosion margin and material modelling

During the lifetime of a ship, the hull is subjected to corrosion which results in reduced thickness of its structural members. In order to compensate for this effect, corrosion margins are added to the net scantlings, i.e. the gross scantling is the sum of the net scantling and the corrosion margin. The net scantling approach is applied to maintain the required minimum structural strength of a vessel during its whole lifetime.

The corrosion margins of the struck coastal oil tanker are shown in Figure 4. They were estimated from the Common Structural Rules for Bulk Carriers and Oil Tankers (CSR-BC&OT) (IACS 2017). The CSR-BC&OT also gives guidelines how to estimate the thickness reduction of different structural members due to loss of material from corrosion connected to the ship's age. For RoPax vessels, there are no clear guidelines for corrosion margins. In this study, a corrosion margin of 20% has been added on all parts in the double bottom and side-shell structures in accordance with Ringsberg et al. (2017).

It is relevant to relate the reduction of the corrosion margin of a ship to its age. Full reduction of a corrosion margin can, for example, represent 25 years of operation for a vessel. But, the reduction of the corrosion margin is not a linear function of a ship's age since protective coatings lower the corrosion rate in the beginning of a ship's operational life. Paik et al. (2003) found that the influence from corrosion is minor or negligible up to 7.5 years of operation. If one assumes that the corrosion starts after this time, the reduction of the corrosion margin follows a linear relationship with respect to the age of the ship, and that it is independent of the coating's condition and if it is repaired or not, a 50% reduction of the corrosion margin corresponds to around 16 years of operation.

Table 4 presents the relationship between the remaining corrosion margin in intervals and how they correlate with the material model used in the FE analyses. The intervals, obtained from recommendations in CSR-BC&OT (IACS 2017), are relevant for the coastal oil tanker where different parts of the structure have various percentages of loss of material due to corrosion. For the RoPax vessel, where the corrosion margin was assumed to be uniform

Table 4. Corroded material model assignment based on different percentage of corrosion.

Remaining corrosion margin	Material model
100%	Virgin (non-corroded) material
50%–<100%	Minorly corroded
0%–<50%	Severely corroded

and always 20% of the gross scantling, the minorly corroded material corresponds to a reduction of 50% of this margin and the severely corroded material 100% of this margin. Furthermore, in the ship–ship collision simulations, the friction coefficient of corroded surfaces was also altered; see Section 2.4. Corroded surfaces in contact were given a friction coefficient of 0.5, while non-corroded surfaces in contact had a coefficient of friction of 0.3.

2.4. Parametric study

The parametric study was designed to enable systematic analysis of several factors and their influence on the shape and size of the damage opening of the struck ships, and how the ultimate strength was affected by these factors; see Table 5 for the analysis matrix. Status 'intact' refers to ultimate strength analyses of cases where the RoPax and coastal oil tanker were assessed without any damage opening, while status 'damaged' refers to ultimate strength analyses of cases where the vessels have damage openings as calculated by the FE analyses.

Thickness reductions and loss of material due to corrosion of the ship structures were considered in the three corrosion margin cases shown in Table 4 and the material behaviour was varied between the three different material models in Table 3. A 'reference' value of the friction coefficient was set to 0.3 for all non-corroded surfaces; this is a value which is often used in the literature for similar ship–ship collision simulations. An assumed value of 0.5 was used to represent a corroded surface (see Ringsberg et al. (2017), where the influence from friction alone as a parameter was studied in detail). The value of the friction coefficient was altered primarily for the inner corroded surfaces of the ballast tanks in both of the ships, and in the cargo holds of the coastal oil tanker. Moreover, the striking tanker ship speed was 7 knots, and it was always assumed to have full corrosion margin and material characteristics according to the NVA virgin material.

Table 5. Analysis matrix in the parametric study.

Case	Status (I/D)	Ship[a] (T/R)	Material model	Remaining corrosion margin (%)	Friction coefficient (-)
T1-I	Intact	Tanker	Virgin	100	–
T2-I	Intact	Tanker	Virgin	50	–
T3-I	Intact	Tanker	Virgin	0	–
T4-I	Intact	Tanker	Minor	50	–
T5-I	Intact	Tanker	Severe, Minor	0, 50	–
T1-D	Damaged	Tanker	Virgin	100	0.3
T2-D	Damaged	Tanker	Virgin	50	0.5
T3-D	Damaged	Tanker	Virgin	0	0.5
T4-D	Damaged	Tanker	Minor	50	0.5
T5-D	Damaged	Tanker	Severe, Minor	0, 50	0.5
R1-I	Intact	RoPax	Virgin	100	–
R2-I	Intact	RoPax	Virgin	50	–
R3-I	Intact	RoPax	Virgin	0	–
R4-I	Intact	RoPax	Minor	50	–
R5-I	Intact	RoPax	Minor	0	–
R1-D	Damaged	RoPax	Virgin	100	0.3
R2-D	Damaged	RoPax	Virgin	50	0.5
R3-D	Damaged	RoPax	Virgin	0	0.5
R4-D	Damaged	RoPax	Minor	50	0.5
R5-D	Damaged	RoPax	Minor	0	0.5

[a] Tanker refers to the struck coastal oil tanker.

3. Results

3.1. Shape and size of the damage opening

The survivability of a ship in a collision accident (e.g. time to evacuate, time to capsize; see Schreuder et al. 2011) and its ultimate strength depend on the shape, size and location of the damage opening, together with the sea state conditions which affect the flooding of the ship and the loads acting on it. Figure 5 presents the projected shape and size of damage openings of the RoPax ship and the coastal oil tanker from the FE analyses in Table 5. Figure 6 presents the deformed and damaged cross-sections where the damage openings are the largest. Note that these two figures together give an indication of the volume of the damage, which is a crucial parameter with regard to the ultimate strength of the ship.

For the RoPax ship, the shapes of the damage openings are in agreement with Hogström and Ringsberg (2012). The damage

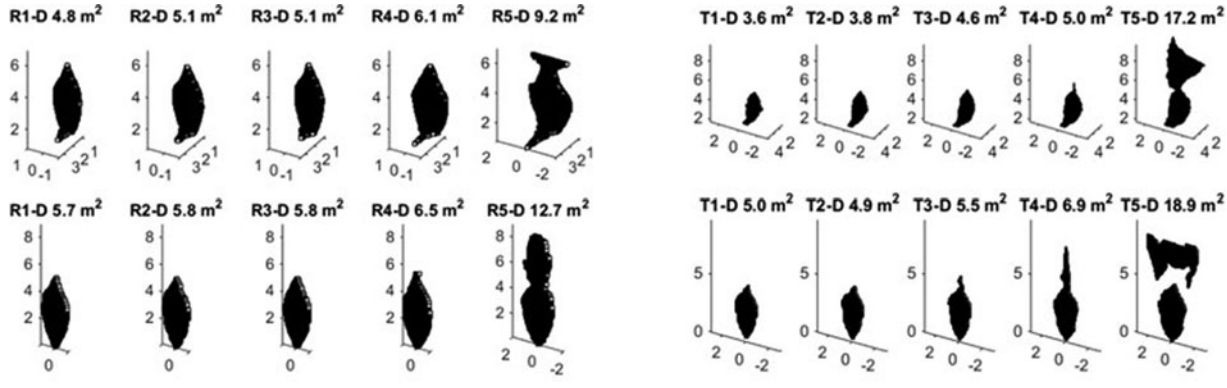

Figure 5. Shape and size of the damage openings for the RoPax (R) and costal oil tanker (T) cases: (upper) inner side-shell and (lower) outer side-shell.

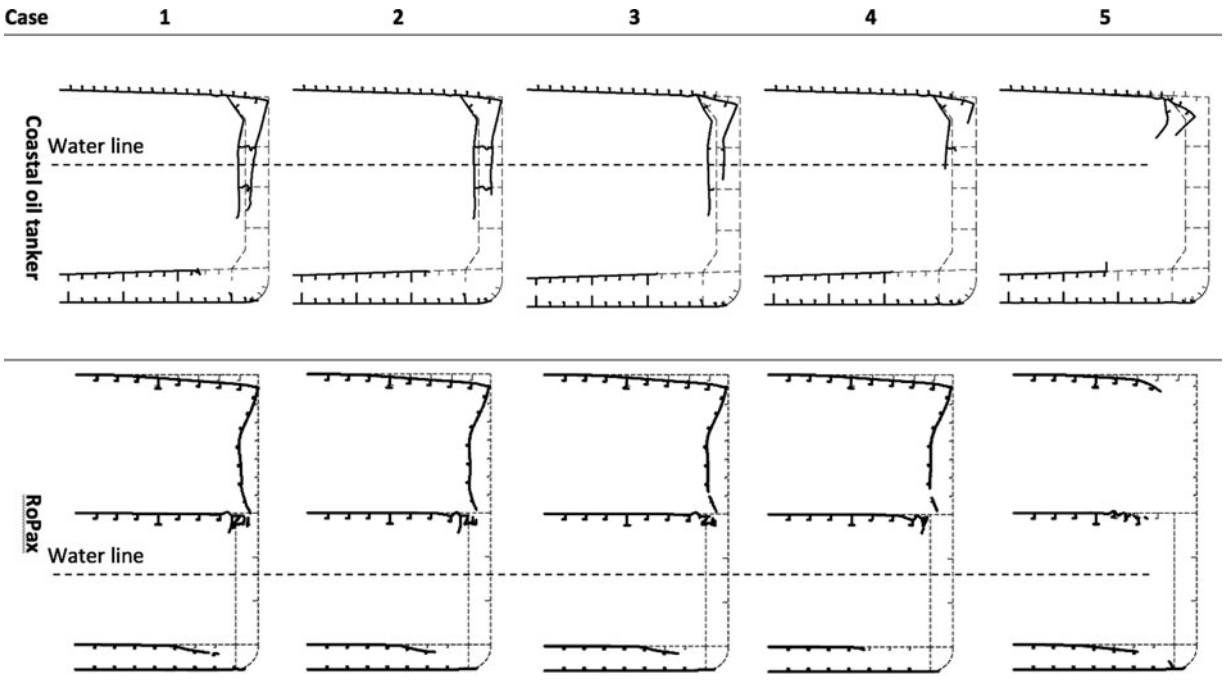

Figure 6. Deformed and damaged cross-sections for the RoPax and costal oil tanker cases.

opening shape on the inner and outer side-shells are rather similar. As expected, the sizes of the damage openings in the inner side-shell are smaller compared to the outer side-shell. It is also found that there is a small increase in size of the damage opening when the corrosion margin is reduced; cf. R1-D and R3-D. There is an influence from the material model which shows that the damage opening is larger when the minorly corroded material model (case R5-D) is used compared with the virgin material model (R3-D). The results show that the increase in damage opening size in the inner side-shell is 92% between a new-built ship (R1-D) and a minorly corroded ship (R5-D).

For the coastal oil tanker, the damage shapes on the inner side-shell shell differ compared to the outer side-shell because the bilge hopper and the inner bottom are damaged in addition to the inner side-shell. The sizes of the damage openings for the coastal oil tanker cases are, for all of the cases except for T5-D, smaller compared to the corresponding RoPax ship cases. It was expected because the ships were impacted by the same striking vessel and the coastal oil tanker has more structural elements with larger dimensions compared with the RoPax ship. Hence, the kinetic energy is dissipated more efficiently in this ship before fracture occurs. For the T5-D case, the influence from corrosion degraded the structure too much to resist the impact load. Further, except for these observations, the same trend was found as for the RoPax ship: a reduction of the corrosion margin results in a larger size of the damage opening, cf. T1-D and T3-D. The material models for minorly and severely corroded materials (T5-D) resulted in larger damage opening compared with the virgin material model (T3-D). The results show that the increase in damage opening size in the inner side-shell is 378% between a new-built ship (T1-D) and a minorly/severely corroded ship (T5-D).

Consequently, the results in the Figure 5 show that crashworthiness analyses of corroded ships involved in collision accidents, where the shape and size of the damage opening is of interest, should be carried out considering a reduction of the corrosion margin, a constitutive material model representative for the corroded materials and friction conditions of corroded surfaces. If these factors are not considered, the size of the damage opening will be underestimated (i.e. the crashworthiness will be overestimated) and the ultimate strength will be overestimated (see Section 3.3).

3.2. Energy analysis

The internal energy is comprised of the elastically stored energy, and the dissipated energies from plastic deformation and damage. Figure 7 presents the friction energy (F) and the total internal energies of the striking tanker ship (IE_1) and the struck ship (IE_2) at the end of each FE analysis. The sum of these energies corresponds to the total kinetic energy of the striking tanker at the outset of an analysis: 70.0 MJ. For the RoPax ship, it was found that these energies vary little between the cases R1-D to R4-D, which was a bit surprising. However, case R5-D – with no remaining corrosion margin, the minorly corroded material model and the high value of the friction coefficient – has the lowest internal energy for the striking ship among the cases studied. For this case, the internal energy of the struck ship and the friction energy have increased. For the coastal oil tanker, the results are similar but they show more clearly how the loss of corrosion margin, the consideration of corrosion material models and friction coefficient on corroded surfaces, affect the collision resistance of the struck ship negatively.

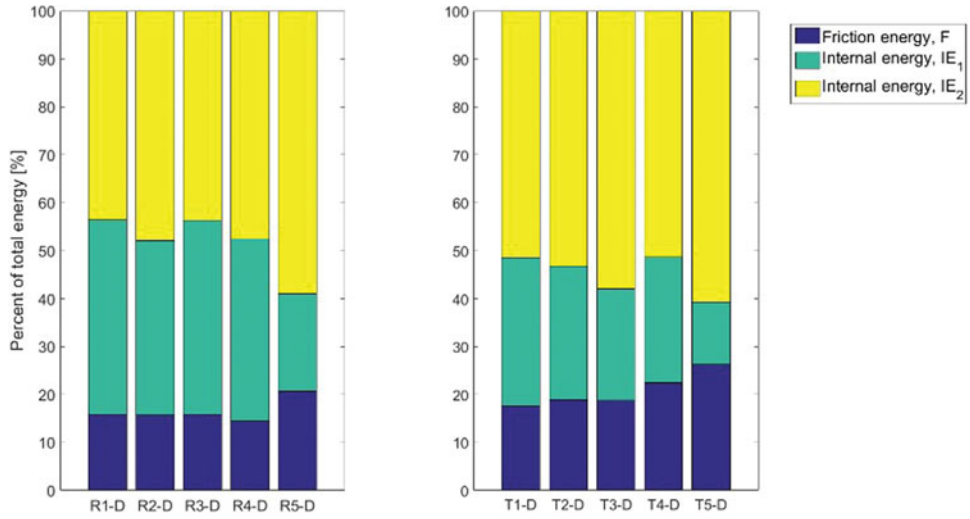

Figure 7. Per cent of total energy at the end of each FE analysis divided into friction energy (*F*), total internal energies of the striking tanker ship (bow) (IE_1) and the struck ship (side-shell) (IE_2): (left) the RoPax ship, and (right) the coastal oil tanker. (This figure is available in colour online.)

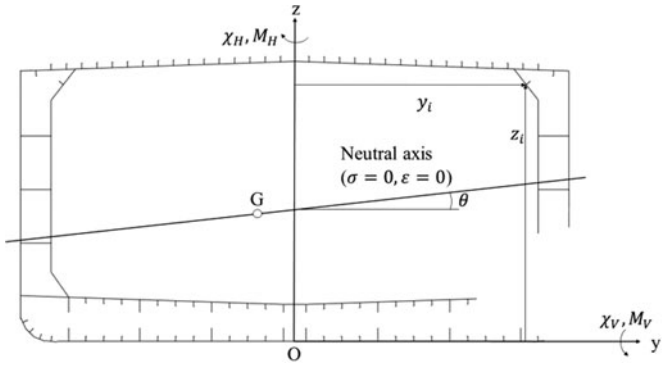

Figure 8. Illustration of the neutral axis position, centroid (*G*) and direction of loading (M_H and M_V) for an asymmetrically damaged cross-section.

3.3. Ultimate and residual strength analyses

The ultimate strength analyses were carried out using the Smith method in Fujikubo et al. (2012) and limited to vertical bending in the current study. It has proved to be a practical approach with satisfactory engineering accuracy and is therefore commonly accepted for assessment of the ultimate strength due to vertical and horizontal bending moments. This Smith method was implemented in an in-house MATLAB code; all details concerning the development of the code can be found in Kuznecovs and Shafieisabet (2017). It was developed for the analysis of both undamaged and damaged ship hulls. Figure 8 shows an illustration for a damaged ship hull of how the code takes into account for the rotation and the displacement of the neutral axis (NA) during the analysis. The code was verified with good agreement for undamaged ship hull cross-sections against large number of cases taken from the literature, such as from Nishihara (1984) who carried out experiments, and Downes et al. (2016) who carried out numerical simulations using the FE method. All verification cases were also modelled and analysed using the commercial software MARS2000 (Bureau Veritas 2015). Results from the ultimate strength analyses of undamaged ships (i.e. intact conditions in Table 5) are presented in Section 3.3.1.

Yamada (2014) presented a residual strength index, RSI2 = M_U/M_P, to show the dependence of ultimate strength due to age for intact corroded vessels without collision damage; M_U is the ultimate vertical bending moment, M_P is the ultimate fully plastic bending moment. In the current study, the residual strengths of the undamaged and damaged hull structures were calculated and assessed with respect to the same reference axis which was in parallel to the water surface. The calculation of the RSI2 index for different material conditions (virgin and corroded) and corrosion margin reduction models was used to show how the RSI2 decreases as the corrosion margin decreases and the material's properties degrade. This means that the loss in structural integrity is proportional to the age of the ship structure. The results are presented in Section 3.3.2.

3.3.1. Intact conditions

The ultimate strength for intact conditions of the RoPax ship and the coastal oil tanker were calculated for all 'intact' cases presented in Table 5. The results for the RoPax vessel are presented in Figure 9 as the ultimate vertical bending moment, M_U, and the vertical position of the NA versus the curvature, χ. The ultimate vertical bending moment for R1-I was calculated to 615 and −563 MNm in hogging and sagging, respectively. The ultimate strength in sagging condition was governed by buckling collapse of the upper and main decks, while in the hogging condition it was determined by buckling of the double bottom structure. The other curves in the figure show how the M_U in hogging and sagging are reduced due to corrosion, and how the location of the NA is translated in the vertical direction.

Figure 10 presents the $M_U - \chi$ and NA $- \chi$ results for the coastal oil tanker. The M_U in hogging and sagging was calculated to 1.42 and −1.02 GNm for T1-I, respectively. The higher ultimate vertical bending moment in hogging condition was mainly due to the stiffness contribution from the double bottom structure. The reduction in ultimate load capacity during

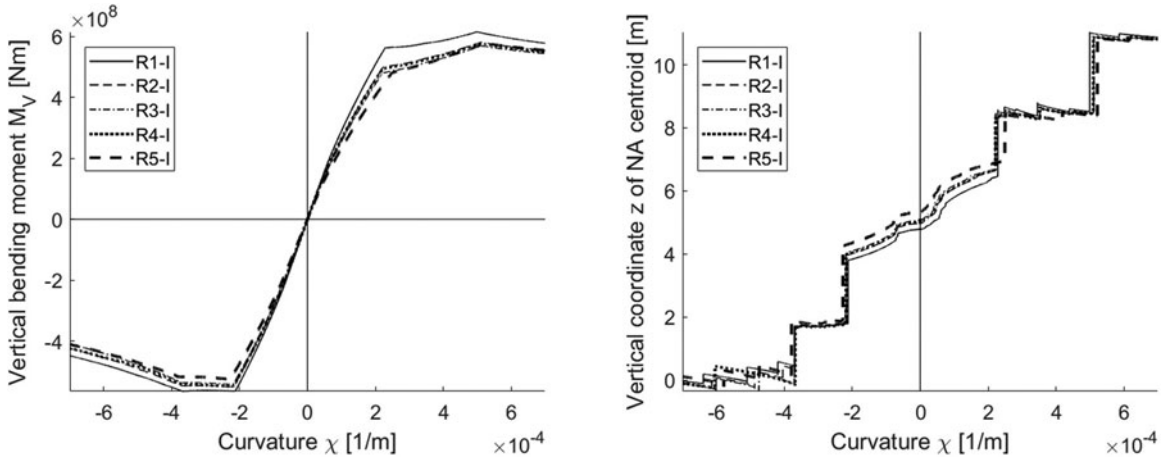

Figure 9. Ultimate strength analysis of the undamaged (intact) RoPax ship: (left) vertical bending moment versus curvature, and (right) NA versus curvature.

sagging condition at the curvature $\chi = -0.20 \times 10^{-3}$ m^{-1} was caused by buckling of the strength deck; this resulted in a rapid shift of the NA towards the baseline. In hogging condition at the curvature $\chi = 0.26 \times 10^{-3}$ m^{-1}, the reduction in ultimate strength occurred due to buckling of the double bottom stiffener elements.

3.3.2. Damaged conditions

Figure 11 presents the $M_U - \chi$ results for the RoPax ship and the coastal oil tanker for the 'damaged' cases in Table 5. For the RoPax ship, the M_U reduction in hogging and sagging, between R1-D and R5-D, is 21% and 15% respectively. For the coastal oil tanker, the same analysis between T1-D and T5-D shows

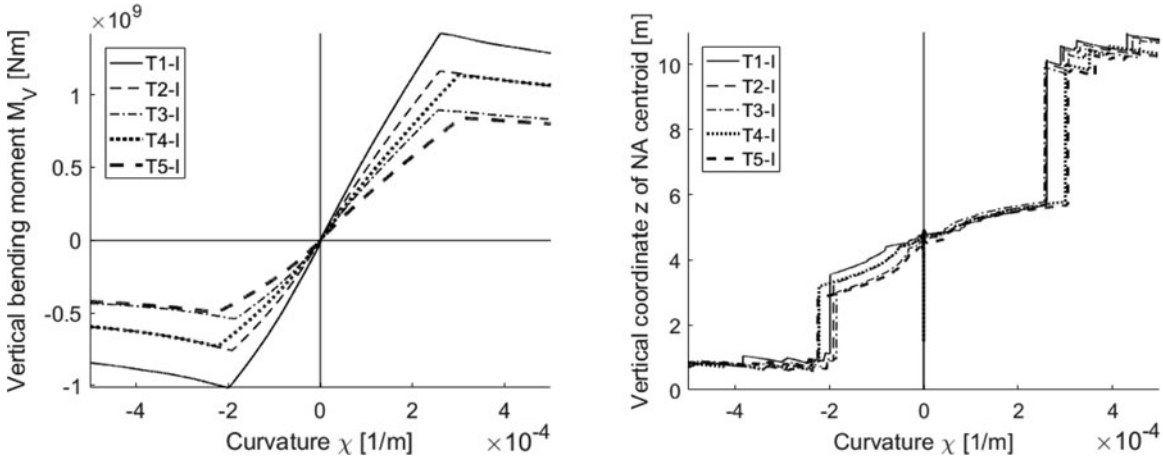

Figure 10. Ultimate strength analysis of the undamaged (intact) costal oil tanker: (left) vertical bending moment versus curvature, and (right) NA versus curvature.

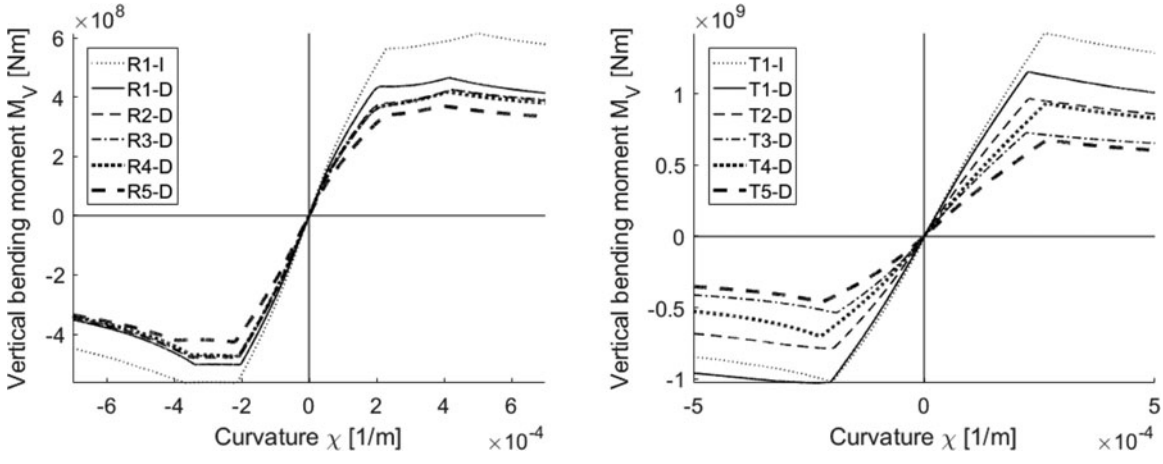

Figure 11. Ultimate strength analysis of damaged vessels presented as vertical bending moment versus curvature: (left) the RoPax ship, and (right) the coastal oil tanker.

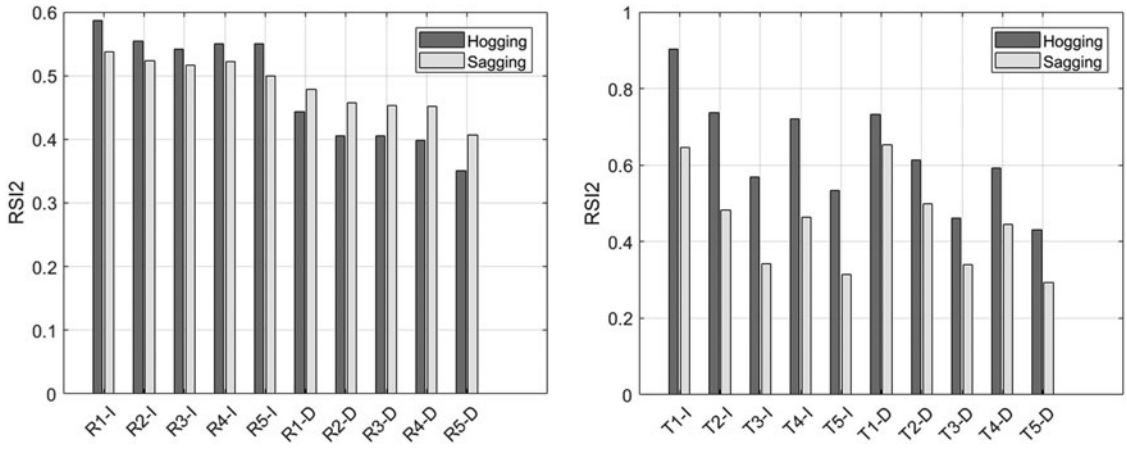

Figure 12. RSI2 for the (left) RoPax ship, and (right) the costal oil tanker.

a reduction by 41% and 55% in hogging and sagging, respectively. A larger reduction in hogging was expected since the damage opening is on the compression side. Detailed analyses of the results show that the rotation and displacement of the NA resulted in collapse modes (elasto-plastic collapse, plate buckling, torsion buckling, beam column buckling) which led to a larger reduction in M_U in sagging compared to hogging for the current vessel and damage cases.

The results in Section 3.1 show that the damage opening of the coastal oil tanker was smaller for all cases but one (T5-D) compared to the RoPax ship. The larger percentage in reduced ultimate strength between the two vessels is because of two interacting reasons. First, the tanker's ultimate strength is affected more by corrosion compared to the RoPax ship, cf. Figures 9 and 10 for intact conditions. Second, the Smith method in Fujikubo et al. (2012) shall be applied in the cross-section where most of the structure's elements are removed because of the collision damage. This means that the shape of the damage opening and its location are important. A comparison of the damage shapes in the outer and inner side-shells in Figure 5 shows that the expansion or 'lengths' of the damages, i.e. along the side-shell, bilge corner and double bottom, are quite similar. However, the damage openings in the coastal oil tanker are in locations where the structural elements contribute significantly to the moment of inertia and structural strength; the RoPax ship is obviously less sensitive to this in its structural design.

The residual ultimate strength in damaged condition was calculated in the cross-section that had the largest damage expansion (see above and Figure 6) in the FE analysis. The residual strength index RSI2 according to Yamada (2014) was used in the assessment which compared all the damaged and the intact cases in Table 5. Figure 12 presents the results in hogging and sagging conditions. For the coastal oil tanker, the RSI2 value was always lower in sagging compared to hogging, independent of if the ship was intact or damaged. For the RoPax ship, the index was almost the same in hogging and sagging for the intact cases, but for all damaged cases a larger value was found in sagging compared to hogging. Thus, this ship type suffers more from the collision damage and corrosion with respect to the relationship between hogging and sagging RSI2 values, even if it is relatively constant between the cases R1-D to R5-D. For the coastal oil tanker, there is a significant reduction in the RSI when comparing the T3-D and T5-D cases with most of the other coastal oil tanker cases. It is also notable that the coastal oil tanker has significantly larger reduction in RSI2 values between its cases compared to the RoPax ship's cases.

Figure 13 presents diagrams which illustrate how the RSI2 index is changed for intact and damaged ships which have different corrosion conditions in the model; see Table 5 for details regarding the material model and friction coefficient for each case. The residual ultimate strength capacity is decreased for both ships as the corrosion margin is reduced, corrosion material models are used and the friction coefficient is adapted to corroded surfaces in contact. A comparison between the cases R3-I and R5-I, as well as R3-D and R5-D, shows how important it is to use an appropriate material model for the corroded material. This is also true for the coastal oil tanker; however, the reduction in corrosion margin has larger influence on the RSI2 value for this ship type.

4. Conclusions

This study contributed to the numerical analysis of ALS and ULS of struck, corroded ships that have been damaged during a ship–ship collision accident. The objective was to study the combined effects of ship–ship collision, and progressive deterioration due to corrosion, on the ultimate strength of aged/corroded ships which were collided by another vessel. Two case study vessels, a RoPax ship and a coastal oil tanker, were investigated when they were struck by a coastal tanker. Explicit FE analyses of collision events were presented where the consideration of corroded ship structure elements, their material characteristics in the model and vessel type were varied systematically in a parametric study. The ultimate strength of the struck ship, for each collision event, was calculated using a verified in-house MATLAB code of the Smith method which used the shape and size of the damage openings from the ship–ship collision FE analyses. The following major conclusions can be drawn from this study.

The crashworthiness of the side-shell structures was reduced when the corrosion margin was reduced, i.e. the size of the damage opening increased. The size of the damage opening

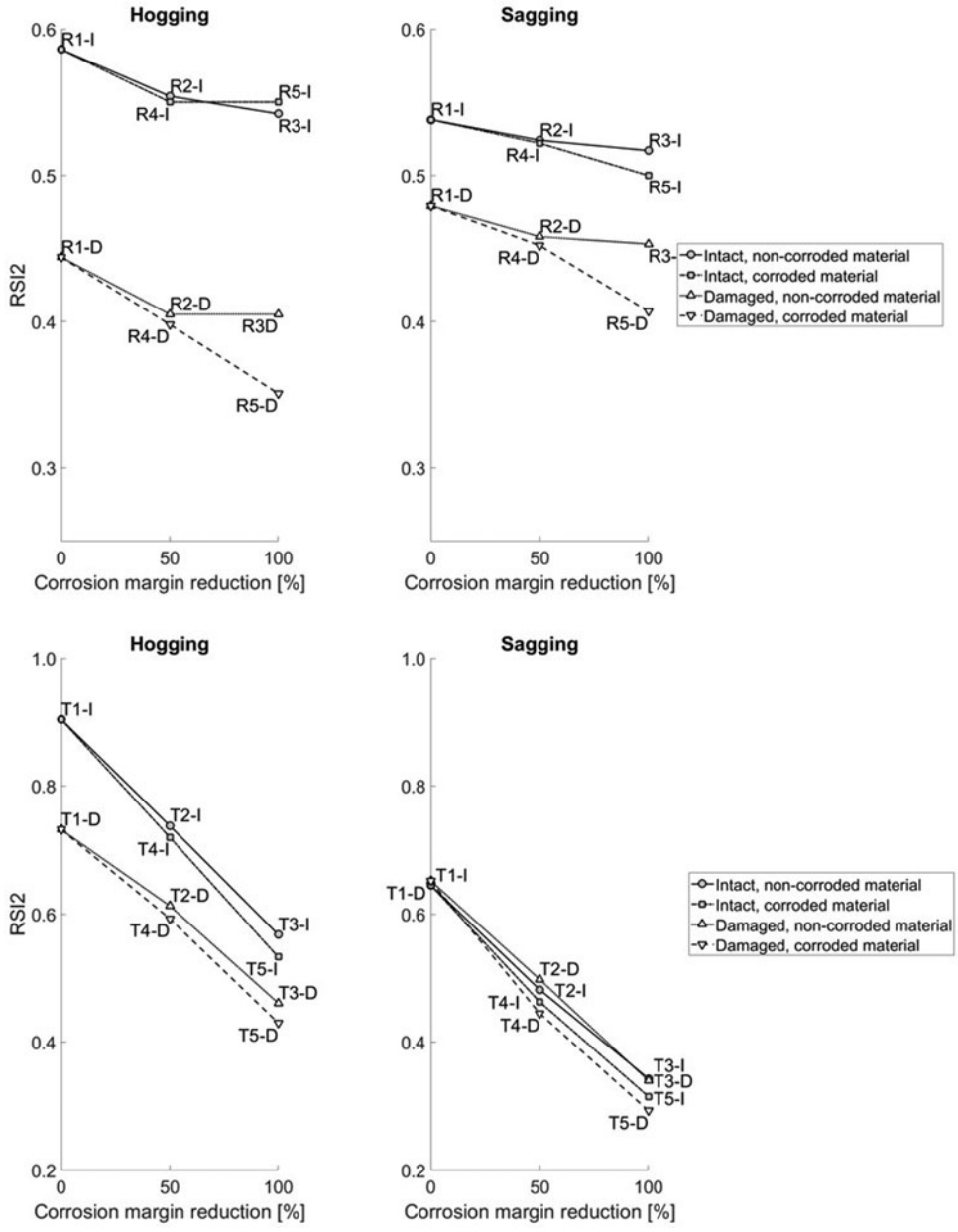

Figure 13. RSI2 index versus corrosion margin: (upper) the RoPax ship, and (lower) the coastal oil tanker.

increased even more when corroded material properties were considered in the analysis. It was found that an assessment of corroded ships involved in collision accidents should be carried out considering a reduction of the corrosion margin and modelling of corroded material properties, otherwise the damage opening may be greatly underestimated.

For a collision-damaged (struck) vessel, a prediction of the reduction in ultimate strength capacity must be carried out taking into account the status of its corrosion margin and the corroded material properties of the structure's material. It was found in the ultimate strength analyses that not only the size of the damage opening is important, but also its location and shape (here, largest expansion in a cross-section) are very important. The results show that this is also dependent on the ship type: the coastal oil tanker suffered from a larger reduction in ultimate strength compared to the RoPax ship due to its structural design. Thus, in ultimate strength analyses of struck and corroded ships, it is recommended to carry out explicit nonlinear FE analyses of the ship collision scenarios in order to as realistically as possible estimate the damage openings' characteristics which are needed in e.g. the Smith method.

The ships' residual strength was quantified by the RSI2 index. For the damaged RoPax ship, the index was reduced significantly when a constitutive model for corroded material was used, while for the tanker, it was affected (reduced) more by the loss of the corrosion margin. Since either the corrosion material model or the corrosion margin affected the value of the RSI2 index the most for the two ship types, it is concluded that the following three factors must always be included in the ALS and ULS of aged, struck ships: a constitutive model for the corroded material, a model for the reduction the corrosion margin, and

finally, a friction coefficient representative for corroded metal surfaces.

Acknowledgments

The FE analyses carried out in this study were partly performed on resources at Chalmers Centre for Computational Science and Engineering (C3SE www.c3se.chalmers.se) provided by the Swedish National Infrastructure for Computing (SNIC).

Disclosure statement

No potential conflict of interest was reported by the authors.

ORCID

Jonas W. Ringsberg http://orcid.org/0000-0001-6950-1864

References

Abaqus. 2016. Dassault systemes simulia, Abaqus version 6.13-3. [accessed 2018 January]. http://www.3ds.com/products-services/simulia/products/abaqus/

AbuBakar A, Dow RS. 2016. The impact analysis characteristics of a ship's bow during collisions. Proceedings of the 7th International Conference on Collision and Grounding of Ships and Offshore Structures (ICCGS 2016); Jun 15–18; Ulsan (Korea): The Society of Naval Architects of Korea (SNAK).

Bureau Veritas. 2015. MARS2000. [accessed 2018 January]. http://www.veristar.com/

Campanile A, Piscopo V, Scamardella A. 2015. Statistical properties of bulk carrier residual strength. Ocean Eng. 106(1):47–67.

Downes J, Tayyar GT, Kvan I, Choung J. 2016. A new procedure for load-shortening and -elongation data for progressive collapse method. Int J Naval Archit Ocean Eng. 9(6):705–719.

Ehlers S. 2010. The influence of the material relation on the accuracy of collision simulations. Mar Struct. 23(4):462–474.

Ehlers S, Østby E. 2012. Increased crashworthiness due to arctic conditions – the influence of sub-zero temperature. Mar Struct. 28(1):86–100.

Faisal M, Noh SH, Kawsar MRU, Youssef SAM, Seo JK, Ha YC, Paik JK. 2016. Rapid hull collapse strength calculations of double hull oil tankers after collisions. Ships Offshore Struct. 12(5):624–639.

Fujikubo M, Zubair MA, Takemura K, Iijima K, Oka S. 2012. Residual hull girder strength of asymmetrically damaged ships. J Japan Soc Naval Archit Ocean Eng. 16:131–140.

Garbatov Y, Guedes Soares C, Parunov J, Kodvanj J. 2014. Tensile strength assessment of corroded small scale specimens. Corros Sci. 85(1):296–303.

Garbatov Y, Parunov J, Kodvanj J, Saad-Eldeen S, Guedes Soares C. 2016. Experimental assessment of tensile strength of corroded steel specimen subjected to sandblast and sandpaper cleaning. Mar Struct. 49(1):18–30.

Hogström P, Ringsberg JW. 2012. An extensive study of a ship's survivability after collision – a parameter study of material characteristics, non-linear FEA and damage stability analyses. Mar Struct. 27(1):1–28.

Hogström P, Ringsberg JW. 2013. Assessment of the crashworthiness of a selection of innovative ship structures. Ocean Eng. 59(1):58–72.

Hogström P, Ringsberg JW, Johnson E. 2009. An experimental and numerical study of the effects of length scale and strain state on the necking and fracture behaviours in sheet metals. Int J Impact Eng. 36(10–11):1194–1203.

[IACS] International Association of Classification Societies. 2017. Common structural rules for bulk carriers and oil tankers. Version: 1 January, 2017. London (UK): International Association of Classification Societies (IACS).

Karlsson U. 2009. Improved collision safety of ships by an intrusion-tolerant inner side-shell. Mar Technol. 46(3):165–173.

Kuznecovs A, Shafieisabet R. 2017. Analysis of the ultimate limit state of corroded ships after collision [MSc thesis report X-17/376]. Gothenburg: Department of Mechanics and Maritime Sciences, Chalmers University of Technology.

Marinatos JN, Samuelides MS. 2015. Towards a unified methodology for the simulation of rupture in collision and grounding of ships. Mar Struct. 42(1):1–32.

Nishihara S. 1984. Ultimate longitudinal strength of mid-ship cross section. Naval Archit Ocean Eng. 22:200–214.

Paik JK, Kim DK, Kim M-S. 2009. Ultimate strength performance of Suezmax tanker structures: pre-CSR versus CSR designs. Int J Mar Eng. 151(A2):39–58.

Paik JK, Kim BJ, Seo JK. 2008. Methods for ultimate limit state assessment of ships and ship-shaped offshore structures: part II stiffened panels. Ocean Eng. 35(2):271–280.

Paik JK, Lee JM, Park YI, Hwang JS, Kim CW. 2003. Time-variant ultimate longitudinal strength of corroded bulk carriers. Mar Struct. 16(8):567–600.

Paik JK, Melchers RE. 2008. Condition assessment of aged structures. Cambridge (England): Woodhead Publishing Limited and CRC Press LLC.

Ringsberg JW, Li Z, Johnson E. 2017. Performance assessment of crashworthiness of corroded ship hulls. Proceedings of the 6th International Conference on Marine Structures; May 8–10; Lisbon (Portigal): CRC Press, Taylor & Francis Group.

Saad-Eldeen S, Garbatov Y, Guedes Soares C. 2011. Experimental assessment of the ultimate strength of a box girder subjected to severe corrosion. Mar Struct. 24(4):338–357.

Samuelides MS. 2015. Recent advances and future trends in structural crashworthiness of ship structures subjected to impact loads. Ships Offshore Struct. 10(5):488–497.

Schreuder M, Hogström P, Ringsberg JW, Johnson E, Janson C-E. 2011. A method for assessment of the survival time of a ship damaged by collision. SNAME J Ship Res. 55(2):86–99.

Storheim M, Alsos HS, Hopperstad OS, Amdahl J. 2015. A damage-based failure model for coarsely meshed shell structures. Int J Impact Eng. 83(1):59–75.

Storheim M, Amdahl J, Martens I. 2015. On the accuracy of fracture estimation in collision analysis of ship and offshore structures. Mar Struct. 44(1):254–287.

Yamada Y. 2014. Numerical study on the residual ultimate strength of hull girder of a bulk carrier after ship-ship collision. Proceedings of the ASME 33rd International Conference on Ocean, Offshore and Arctic Engineering (OMAE2014); Jun 8–13; San Francisco (CA): The American Society of Mechanical Engineers (ASME).

Zhang S, Pedersen PT. 2017. A method for ship collision damage and energy absorption analysis and its validation. Ships Offshore Struct. 12(sup1):S11–S20.